Liquid Crystals
Publication details, including instructions for authors and subscription information:
http://www.informaworld.com/smpp/title~content=t713926090

Metallomesogens: enaminoketone derivatives of the 3-oxa, 3-thia- and 3-selena-butyric amides

Jadwiga Szydłowska[a]; Andrzej Jurkiewicz Corresponding author[a]; Adam Krówczyński[a]
[a] Department of Chemistry, Laboratory of Dielectrics and Magnetics, 02-089 Warsaw, Poland

Online publication date: 12 May 2010

To cite this Article Szydłowska, Jadwiga , Jurkiewicz Corresponding author, Andrzej and Krówczyński, Adam(2004) 'Metallomesogens: enaminoketone derivatives of the 3-oxa, 3-thia- and 3-selena-butyric amides', Liquid Crystals, 31: 12, 1655 — 1662
To link to this Article: DOI: 10.1080/02678290412331316002
URL: http://dx.doi.org/10.1080/02678290412331316002

LIQUID CRYSTALS, VOL. 31, NO. 12, DECEMBER 2004, 1655–1662

Metallomesogens: enaminoketone derivatives of the 3-oxa, 3-thia- and 3-selena-butyric amides

JADWIGA SZYDŁOWSKA, ANDRZEJ JURKIEWICZ* and ADAM KRÓWCZYŃSKI

Department of Chemistry, Laboratory of Dielectrics and Magnetics, Warsaw University, Al. Żwirki i Wigury 101, 02-089 Warsaw, Poland

(*Received 9 June 2004; accepted 18 August 2004*)

Liquid crystalline Ni(II) and Cu(II) complexes of tetradentate ligands, enaminoketones and 3-oxa; 3-thia- and 3-selena-butyramides were synthesized and examined. The compounds show very low C_1 symmetry resulting from the chiral donor atoms — oxygen, sulphur and selenium — incorporated in the butyric amide moiety. This chirality can be observed in NMR studies. The complexes exhibit enantiotropic as well as monotropic calamitic SmA and N phases.

1. Introduction

Metallomesogens may be easily designed to form columnar as well as calamitic phases [1]. The metallic centre is most often coordinated in a planar tetragonal configuration [2, 3] and more rarely in a linear [4] or octahedral environment [5]. The donor atoms usually belong to different monodentate [4, 6], bidentate [5] and tetradentate [2, 3] ligands. The molecules can adopt disc-like or rod-like shapes, although, in some metallomesogens the broad chelating centre disrupts the elongated molecular shape, which in turn influences the appearance of calamitic phases.

Chelating ligands used previously [2, 3] have included the very stable tetradentate enaminoketone compounds containing, in their flat chelating centre, nitrogen and oxygen atoms (see scheme 1). This centre has been used as a mesogenic core in a variety of substances that show calamitic or columnar phases. When two phenyl rings are substituted symmetrically to the enaminoketone centres at both ketone carbon atoms, a mesogenic core of C_{2v} symmetry is formed, see scheme 1(*a*) [2]. For such Ni(II) and Cu(II) complexes rod-like or disc-like mesophases appear and the type of liquid crystalline phase depends on the number of terminal alkyl and/or alkoxy chains substituted at the phenyl rings which determine the molecular shape. When only one phenyl ring is attached to the tetradentate enaminoketone centre at one of the carbonyl groups, elongated Ni(II) and Cu(II) complexes of C_s symmetry are created, or the symmetry is lowered to C_1 for the non-coplanar oxovanadium(IV) (VO) ion, see scheme 1(*b*) [3]. These molecules contain a protruding enaminoketone hexagonal ring giving a relatively wide metallic centre and thus only rather weakly promoting calamitic behaviour. Such substances exhibit calamitic phases with only narrow temperature ranges.

In this work, we examined compounds with a slightly enhanced calamitic molecular anisotropy in which the protruding moiety has been replaced by a smaller five-membered ring. In the metallomesogens synthesized (series I–IV) the nickel(II) or copper(II) ions are complexed by two nitrogen atoms coming from the diaminobenzene moiety (scheme 2). As for the remaining donor atoms, one of them, an oxygen atom, belongs to the ketone group while the other is varied and comes from a butyric moiety. Specifically, this is either oxygen (series I), sulphur (series II and III) or selenium (series IV). It has sp^3 orbital hybridization. With substitution by the methyl group, which may be directed below or above the molecular plane, the donor atom is considered to be an asymmetric centre yielding C_1 molecular symmetry [7]. The molecular shape is extended by alkoxy chains attached at the *para*-position of the diaminobenzene ring, as well as by various substituents attached to the carbonyl group, i.e. an alkyl chain in series I, II, IV or a substituted phenyl ring in series III. The complexes exhibit nematic and smectic A calamitic phases which are enantiotropic as well as monotropic in nature.

2. Experimental

2.1. *Synthesis*

The synthetic procedure for the target complexes is shown in scheme 2 [2, 3]. The starting materials are well

*Author for correspondence; e-mail: jurand@chem.uw.edu.pl

Liquid Crystals ISSN 0267-8292 print/ISSN 1366-5855 online © 2004 Taylor & Francis Ltd
http://www.tandf.co.uk/journals
DOI: 10.1080/02678290412331316002

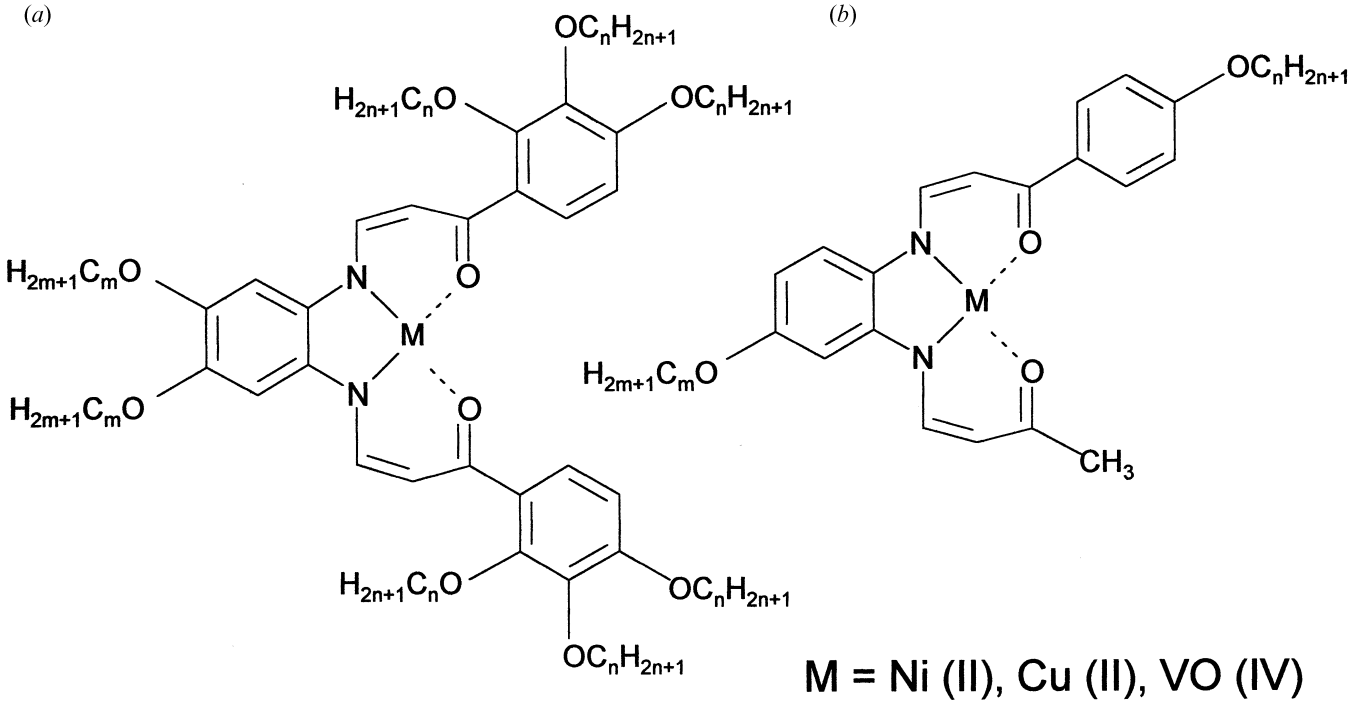

Scheme 1. Enaminoketone derivatives having (*a*) C_{2v} symmetry [2] and (*b*) C_s symmetry [3].

known and their syntheses are routine. Starting from appropriate methyl ketone **1** (1 mmol) and ethyl formate **2** (1.5 mmol) the salt **3** was obtained by the Claisen formylation reaction. The appropriate 4-alkoxy-1,2-phenylenediamine **4** (1 mmol) and a formyl ketone derivative **3** (1 mmol) dissolved in methanol (50 ml), were neutralized with acetic acid (to pH about 6) and reacted at room temperature. This reaction proceeds selectively at the 1-amino group because of its increased nucleophilic properties over the 2-amino group. This effect results from the electrodonating influence of the alkoxy substituent on its *para*-position, which leads to a crystalline intermediate compound **5**. This was purified by recrystallization from octane (yield 70–80%). The remaining amino group of the obtained product **5** (1 mmol), reacts with 3-oxa-, 3-thia- or 3-selena-butyric chloride (1 mmol) to give the ligands **6** (yield 60–70%). The solutions of the ligands **6** (1 mmol) were heated under reflux for 5 min with the metal acetate $M(OAc)_2H_2O$ (1.1 mmol) in MeOH (5 cm^3); precipitates of the appropriate complexes were formed during cooling. They were crystallized from octane (yields in all cases were about 50–60%). The elemental C, H and N analyses for the complexes were satisfactory.

2.2. *NMR spectra*

The NMR spectra (in $CDCl_3$) of the compound **5**, and the Ni(II) complexes were obtained (Varian UNITY plus 500 MHz). They are consistent with the assumed structures with no sign of additives or impurities. Some examples are now quoted.

^{1}H NMR for **5** ($n=9$, $m=8$): $\delta=0.85$–0.92 (m, 6H, CH_3); 1.20–1.80 (m, 26H, CH_2 without OCH_2 and $COCH_2$); 2.38 (t, $J=7.8$ Hz, 2H, $COCH_2$); 3.71 (s, 2H, NH_2); 3.88 (t, $J=6.3$ Hz, 2H, OCH_2); 5.26 (d, $J=7.3$ Hz, H, $COCH=CH$); 6.30–6.34 (m, 2H, aryl); 6.88 (d, $J=8.8$ Hz, H, aryl); 7.03 (dd, $J=7.3$, 11.7 Hz, H, $COCH=CH$); 11.35 (d, $J=11.7$ Hz, H, NH).

^{1}H NMR for I-2 ($n=9$, $m=8$, $A=$O, $M=$Ni): $\delta=0.87$–0.91 (m, 6H, CH_3); 1.20–1.76 (m, 26H, CH_2 without OCH_2 and $COCH_2$); 2.20 (t, $J=7.2$ Hz, 2H, $COCH_2$); 3.24 (s, 3H, OCH_3); 3.90 (t, $J=6.6$ Hz, 2H, OCH_2); 4.15 (s, 2H, OCH_2CO); 5.30 (d, $J=6.2$ Hz, H, $COCH=CH$); 6.41 (dd, $J=2.7$, 9.0 Hz, H, aryl); 6.96 (d, $J=6.2$ Hz, H, $COCH=CH$); 7.15 (d, $J=9.0$ Hz, H, aryl); 7.98 (d, $J=2.7$ Hz, H, aryl).

^{1}H NMR for II-3 ($n=9$, $m=8$, $A=$S, $M=$Ni): $\delta=0.86$–0.91 (m, 6H, CH_3); 1.20–1.78 (m, 26H, CH_2 without OCH_2 and $COCH_2$); 2.16–2.22 (t, $J=7.3$ Hz, 2H, $COCH_2$); 2.62 (s, 3H, SCH_3); 3.20 and 3.67 (AB, $J=16.6$ Hz, $SCH^IH^{I'}$); 3.92 (t, $J=6.6$ Hz, 2H, OCH_2); 5.36 (d, $J=6.2$ Hz, H, $COCH=CH$); 6.50 (dd, $J=2.7$, 8.8 Hz, H, aryl); 7.28 (d, $J=8.8$ Hz, H, aryl); 7.45 (d, $J=6.2$ Hz, H, $COCH=CH$); 8.26 (d, $J=2.7$ Hz, H, aryl).

^{1}H NMR for II-3 with 8 drops of C_5D_5N ($n=9$, $m=8$, $A=$S, $M=$Ni): $\delta=0.84$–0.92 (m, 6H, CH_3);

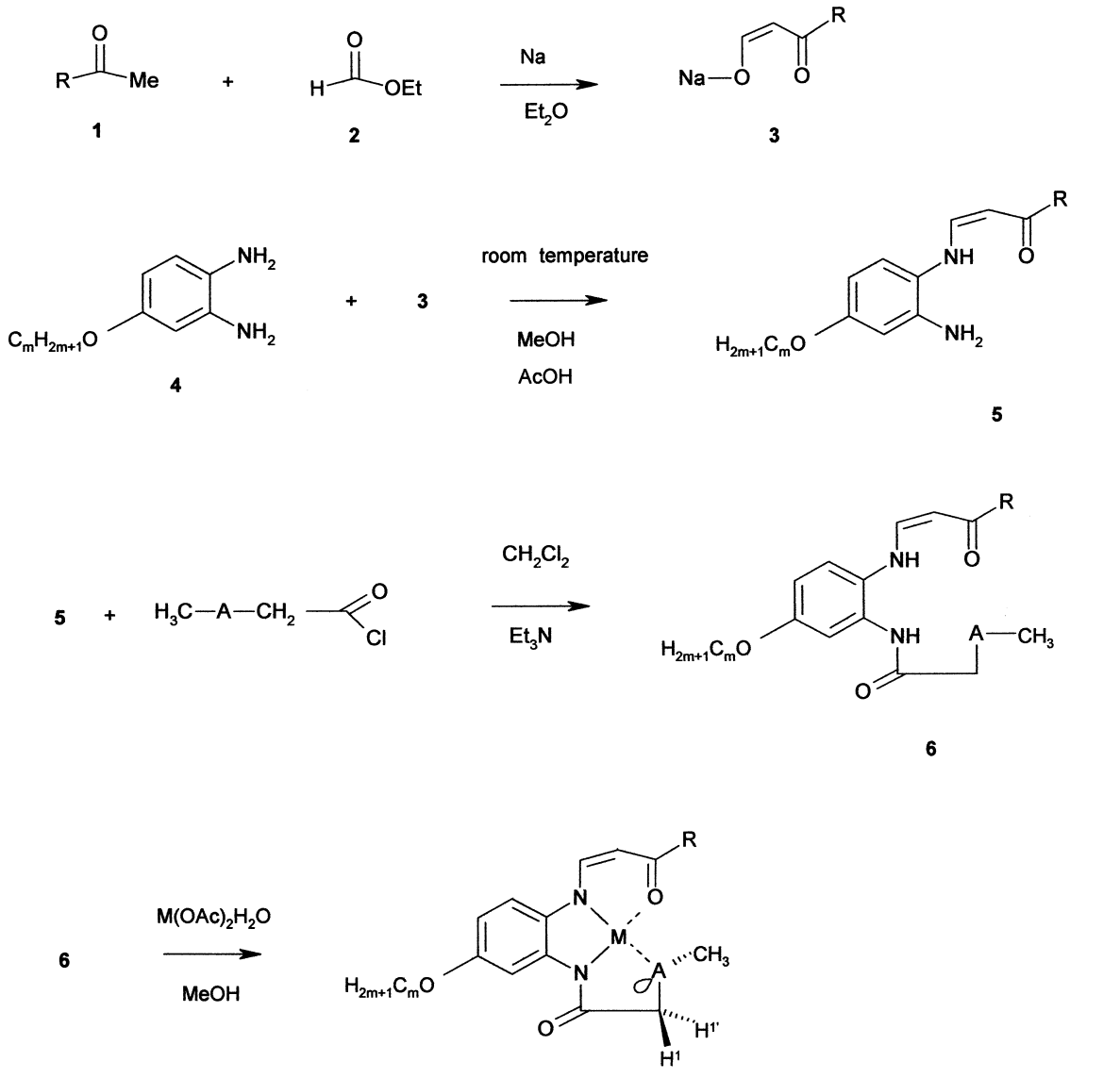

Series I: A=O; M=Ni; R=C_nH_{2n+1}; n=5,8,9,11; m=8,10;

Series II: A=S; M=Ni, Cu; R=C_nH_{2n+1}; n=5,9,11; m=8,10;

Series III: A=S; M=Ni, Cu; R=Ph-OCH_3, Ph-OC_8H_{17}, Ph-(o-OCH_3)-OC_8H_{17}; m=8;

Series IV: A=Se; M=Ni; R=C_nH_{2n+1}; m=8, 10;

Scheme 2. General synthetic route for obtaining the target materials.

1.20–1.78 (m, 26H, CH_2 without OCH_2 and $COCH_2$); 2.18 (t, $J=7.3$ Hz, H CH_2CO); 2.69 (s, 3H, SCH_3); 3.35–3.47 (broad s, 2H, SCH_2); 3.92 (t, $J=6.6$ Hz, 2H, OCH_2); 5.31 (d, $J=6.2$ Hz, H, $COCH=CH$); 6.50 (d, $J=8.8$ Hz, H, aryl); 7.30 (d, $J=8.8$ Hz, H, aryl); 7.93–8.14 (broad s, H, $COCH=CH$); 8.32 (d, $J=2.7$ Hz, H, aryl).

^{1}H NMR for III-6 ($R=$Ph–OCH_3, $A=$S, $M=$Ni): $\delta=0.84$–0.94 (m, 6H, CH_3); 1.20–1.80 (m, 12H, $OCH_2(CH_2)_6CH_3$); 2.67 (s, 3H, SCH_3); 3.19 and 3.66 (AB, $J=16.8$ Hz, 2H, $SCH^1H^{1'}$); 3.80 (s, 3H, $PhOCH_3$); 3.93 (t, $J=6.4$ Hz, 2H, OCH_2); 6.00 (d, $J=6.1$ Hz, H, $COCH=CH$); 6.50 (dd, $J=2.5$, 9.1 Hz, H, aryl); 6.85 (d, $J=8.2$ Hz, 2H, aryl); 7.30 (d, $J=9.1$ Hz, H, aryl);

7.54–7.66 (m, 3H, aryl and COCH=C*H*); 8.28 (d, $J=2.5$ Hz, H, aryl).

^{1}H NMR for III-7 ($R=$Ph–OC_8H_{17}, $A=$S, $M=$Ni): $\delta=0.85$–0.91 (m, 6H, CH_3); 1.24–1.80 (m, 24H, $OCH_2(CH_2)_6CH_3$); 2.69 (s, 3H, SCH_3); 3.21 and 3.69 (AB, $J=16.6$ Hz, 2H, S$CH^1H^{1'}$); 3.91 and 3.98 (two t, $J=6.6$ Hz, 4H, OCH_2); 6.00 (d, $J=6.6$ Hz, H, COC*H*=CH); 6.52 (dd, $J=2.7$, 9.0 Hz, H, aryl); 6.85 and 7.60 (AA'BB', $J=8.8$ Hz, 4H, aryl); 7.63 (d, $J=6.6$ Hz, H, COCH=C*H*); 8.28 (d, $J=2.7$ Hz, H, aryl).

^{1}H NMR for III-8 ($R=$Ph–(o-OCH_3)–OC_8H_{17}, $A=$S, $M=$Ni): $\delta=0.85$–0.92 (m, 6H, CH_3); 1.20–1.80 (m, 24H, $OCH_2(CH_2)_6CH_3$); 2.68 (s, 3H, SCH_3); 3.21 and 3.69 (AB, $J=16.8$ Hz, 2H, S$CH^1H^{1'}$); 3.84 (s, H, OCH_3); 3.92 and 3.98 (two t, $J=6.7$ Hz, 4H, OCH_2); 6.25 (d, $J=6.7$ Hz, H, COC*H*=CH); 6.42 (d, $J=2.1$ Hz, H, aryl); 6.47 (dd, $J=2.1$, 8.8 Hz, H, aryl); 6.52 (dd, $J=2.7$, 9.1 Hz, H, aryl); 7.32 (d, $J=9.1$ Hz, H, aryl); 7.42 (d, $J=8.8$ Hz, H, aryl); 7.63 (d, H, COCH=C*H*, $J=6.7$ Hz); 8.28 (d, $J=2.7$ Hz, H, aryl).

^{1}H NMR for IV-1 ($n=9$, $m=8$, $A=$Se, $M=$Ni): $\delta=0.85$–0.90 (m, 6H, CH_3); 1.20–1.76 (m, 26H, CH_2 without OCH_2 and $COCH_2$); 2.16 (t, $J=6.9$ Hz, 2H, COCH_2); 2.55 (s, 3H, SeCH_3); 3.20 and 3.60 (AB, $J=16.6$ Hz, 2H, Se$CH^1H^{1'}$); 3.90 (t, $J=6.8$ Hz, 2H, OCH_2); 5.35 (d, $J=6.3$ Hz, H, CO*CH*=CH); 6.50 (dd, $J=2.9$, 8.8 Hz, H, aryl); 7.28 (d, $J=8.8$ Hz, H, aryl); 7.45 (d, $J=6.3$ Hz, H, COCH=*CH*); 8.33 (d, $J=2.9$ Hz, H, aryl).

^{1}H NMR for IV-1 with 8 drops of C_5D_5N ($n=9$, $m=8$, $A=$Se, $M=$Ni): $\delta=0.85$–0.92 (m, 6H, CH_3); 1.19–1.77 (m, 26H, CH_2 without OCH_2 and $COCH_2$); 2.15 (t, $J=6.8$ Hz, 2H, COCH_2); 2.57 (s, 3H, SeCH_3); 3.13–3.68 (broad s, 2H, SeCH_3); 3.91 (t, $J=6.8$ Hz, 2H, OCH_2,); 5.30 (d, $J=6.3$ Hz, H, CO*CH*=CH,); 6.50 (dd, $J=2.7$, 8.8 Hz, H, aryl); 7.30 (d, $J=8.8$ Hz, H, aryl); 7.55 (s, H, COCH=C*H*); 8.34 (d, $J=2.7$ Hz, H, aryl).

2.3. *Measurements*

For the identification of the mesophases, microscopic studies of the liquid crystalline textures were performed. A Zeiss Jenapol polarizing microscope, equipped with a Mettler FP 82 HT hot stage was used. Phase transition temperatures were determined by calorimetric measurements performed with a DSC-7 Perkin-Elmer DSC. Thermograms were taken normally at a scanning heating rate 5 K min^{-1}. If necessary, other scanning rates were used and thermal effects were recalculated at a standard rate. X-ray scattering data were obtained from a DRON spectrometer. The EPR spectra were taken in the X-band on a Bruker Elexys 500 spectrometer. For molecular modelling the HYPERCHEM software package was used.

3. Results and discussion

The phase sequences and transition temperatures for the compounds synthesized are summarized in tables 1–4; phase diagrams for series I and II are shown in figures 1 and 2.

Most of the compounds studied show simple mesomorphism, mainly the enantiotropic smectic A phase. In the complexes of series I, as well as two nitrogen atoms binding the metallic nucleus, in the chelating donor centre there are also two oxygen atoms. The liquid crystalline phases exhibited show broad temperature ranges, about 40–70 K. In series II, where the oxygen atom from the butyric moiety is replaced by the sulphur atom, which is larger than the oxygen atom, the temperature range of the liquid crystalline phase is reduced.

Comparing series I and II, the metallomesogens with *para*-decyloxy terminal chains ($m=10$) have similar clearing temperatures, however, the melting points are considerably lower for series I. For both series, shortening the enaminoketone alkyl chain to five carbons gives higher melting and lower clearing temperatures, showing that short substituents at the carbonyl group disrupt the enantiotropic calamitic structure. In series III, for the copper and nickel complexes, lengthening of the mesogenic core by attaching the *para*-octyloxy phenyl ring at the carbonyl group (III-4 and III-7) results in extremely stable

Table 1. Phase transition temperatures (°C) and enthalpy changes (in parenthesis, J g^{-1}) for series I compounds.

Compound	n	m	A	M	Phase sequence
I-1	5	8	O	Ni	Cr–137.4(6.5)–SmA–137.1(6.2)–I
I-2	9	8	O	Ni	Cr–68.2(57.2)–SmA–143.0(11.6)–I
I-3	11	8	O	Ni	Cr–166.6(14.9)–SmA–213[a]–I
I-4	8	10	O	Ni	Cr–68.3(60.4)–SmA–112.9(11.9)–I
I-5	9	10	O	Ni	Cr–68.3(60.4)–SmA–112.9(11.9)–I
I-6	11	10	O	Ni	Cr–61.6(42.2)–SmA–110.0(9.5)–I

[a]From microscopy.

Table 2. Phase transition temperatures (°C) and enthalpy changes (in parenthesis, J g^{-1}) for series II compounds.

Compound	n	m	A	M	Phase sequence
II-1	9	8	S	Cu	Cr–126.5(19,2)–SmA–150.7(8.2)–I
II-2	5	8	S	Ni	Cr 125.6(15.1)–SmA–117.2(1.0)–I
II-3	9	8	S	Ni	Cr–129.7(21.7)–SmA–136,0(8.2)–I
II-4	11	8	S	Ni	Cr–129.7(21.7)–SmA–136,0(8.2)–I
II-5	5	10	S	Ni	Cr–125.5(22.4)–SmA–119.5(1.0)–I
II-6	9	10	S	Ni	Cr–123.6(20.2)–SmA–131.0(6.9)–I
II-7	11	10	S	Ni	Cr–118.1(19.3)–SmA–129.1(6.8)–I

Table 3. Phase transition temperatures (°C) and enthalpy changes (in parenthesis, $J\,g^{-1}$) for series III compounds.

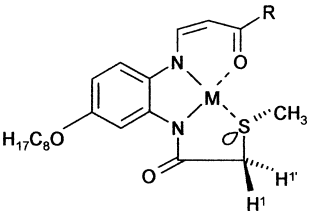

Compound	*R*	*M*	Phase sequence
III-1	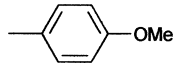	H	Cr–106.8(61.1)–I
III-2	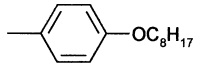	H	Cr–96.9(47.2)[a]–SmA–113.0(5.0)–I
III-3	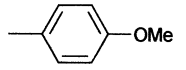	Cu	Cr–186.8(62.2)–SmA–171.7(3.5)–N–172.5(0.4)–I
III-4	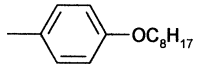	Cu	Cr–155.0(20,8)–SmA–250[b,c]–I
III-5	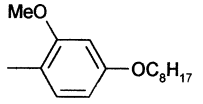	Cu	Cr–151.4(118.2)–SmA–133.6(5.0)–I
III-6	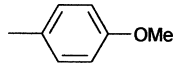	Ni	Cr–191.1(62.6)–SmA–179[b]–I
III-7	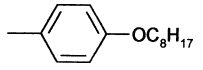	Ni	Cr–174.7(17.6)–SmA–255[b,c]–I
III-8	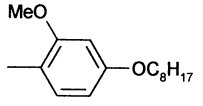	Ni	Cr–127.0(37.2)–SmA–86.3(1.0)–I

[a]Two unresolved peaks.
[b]From microscopy.
[c]Decomposition.

mesogenic calamitic phases with clearing points above their decomposition temperatures (255°C). For example, the copper complex III-4 exhibits a smectic A phase temperature range of 95 K. Replacing the octyloxy chain by the methoxy group in the *para*-position of the phenyl ring dramatically increases the melting temperatures, resulting in monotropic LC phases. Broadening the aroyl group by substitution at the *ortho*-position by the methoxy moiety does not destroy the SmA phase, despite the introduced steric hindrances, however, only a monotropic SmA phase is formed. In series IV containing a selenium chelating atom, the melting and clearing temperatures are similar and a monotropic smectic A phase is observed. The increasing size of the chelating atom in the sequence O, S and Se is accompanied by an increasing melting point that

Table 4. Phase transition temperatures (°C) and enthalpy changes (in parenthesis, $J\,g^{-1}$) for series IV compounds.

Compound	*n*	*m*	*A*	*M*	Phase sequence
IV-1	9	8	Se	Ni	Cr–140.3(43.1)–SmA–137.7(10.4)–I
IV-2	11	10	Se	Ni	Cr–132.3(38.5)–SmA–131.1(10.5)–I

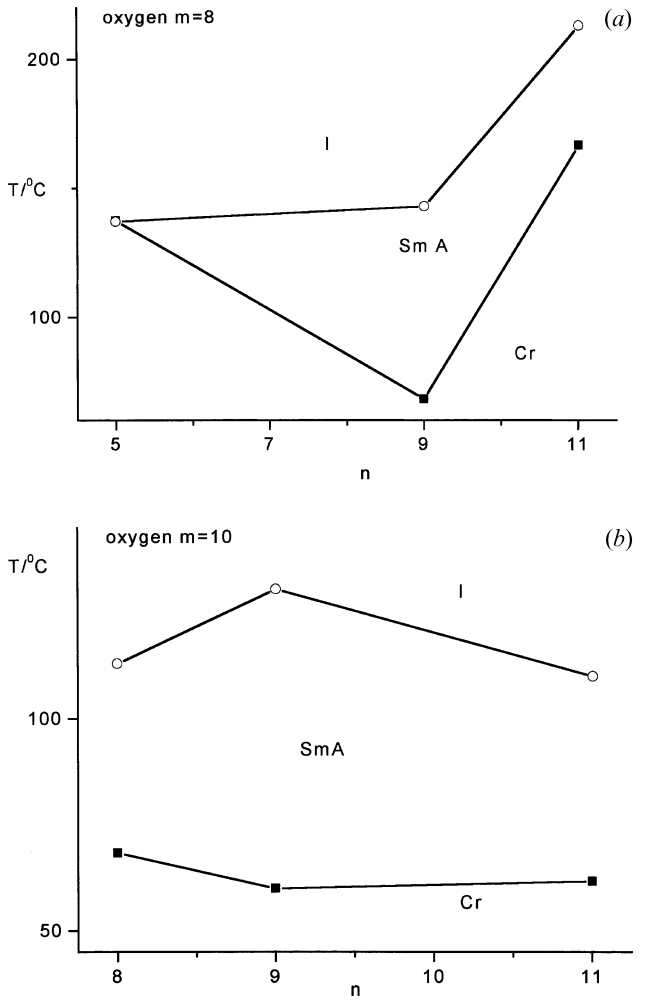

Figure 1. Phase diagram for series I: (*a*) $m=8$, (*b*) $m=10$; full squares are melting and open circles the clearing points.

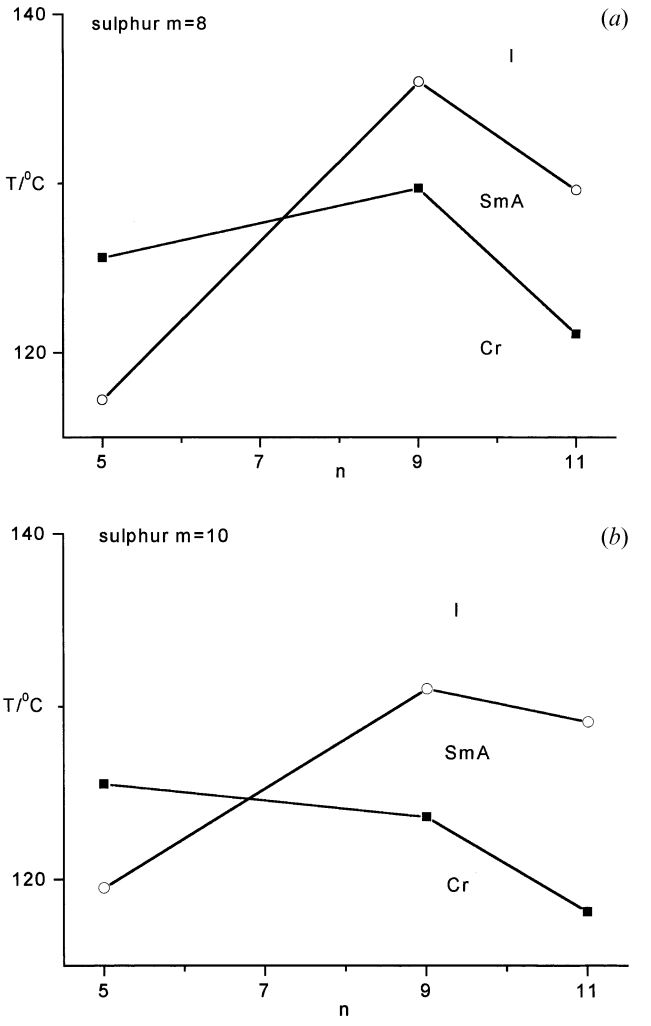

Figure 2. Phase diagram for series II: (*a*) $m=8$, (*b*) $m=10$; full squares are melting and open circles the clearing points.

leads to smaller temperature ranges for the SmA phase. X-ray studies of the SmA phase of the nickel complex I-2, reveals one low angle X-ray signal related to the layer thickness of 25.9 Å. The measured layer thickness is slightly shorter than the molecular length (28.4 Å) estimated from molecular modelling. This shortening is typical for the SmA phases [3].

The potentially asymmetric centres on the chelating atoms belonging to the butyric moiety were confirmed as such by the ^{1}H NMR spectra for sulphur and selenium compounds. The signals arising from protons H^1 and $H^{1'}$ of the methylene group are split giving the AB system indicating that H^1 and $H^{1'}$ are not equivalent. In the case of the oxygen atom, in series I, the chirality is not apparent in the NMR spectrum. This is caused by flipping the orbital configuration of the oxygen atom and changing up and down the position of the methyl group sufficiently quickly to narrow the signals from the non-equivalent geminal protons. Addition of a small amount of pyridine to solutions of sulphur or selenium compounds (series II, III and IV) substantially broadens the NMR signals of the geminal protons. This suggests the breaking of the coordinating bond between the A atom and metallic nucleus, which results in a more frequent inversion of the chiral centre (see scheme 3). On further increasing the

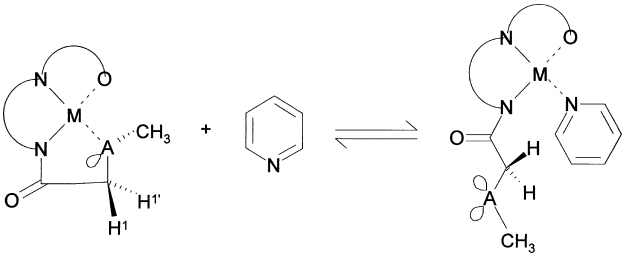

Scheme 3. Reaction of the asymmetric centre with pyridine.

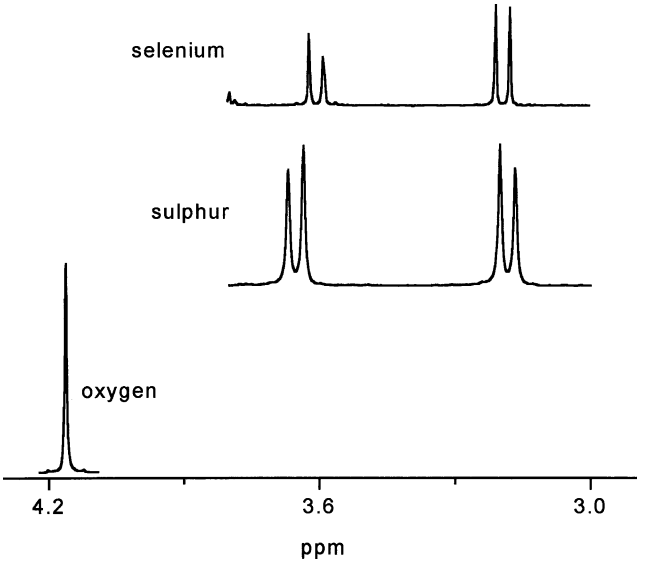

Figure 3. NMR spectra of oxygen (I-2), sulphur (II-3) and selenium (IV-1) compounds dissolved in deuterated chloroform.

pyridine concentration, one sharp peak appears that may suggest the destruction of the chiral centre in this reaction.

The ESR spectra were recorded for the copper complex II-1 containing in the flat chelating centre an asymmetric sulphur atom. This compound dissolved in methylene chloride exhibits four signals at room temperature. The observed hyperfine structure arises from paramagnetic interactions of the copper nucleus ($I=3/2$) with an unpaired copper electron. The peaks at $I=-1/2$ and $-3/2$ in the spectrum reveal additional super hyperfine structure — they are split into many signals as a result of the vicinity of the paramagnetic nitrogen and hydrogen nuclei. The magnetic parameters related to this interaction are shown in figure 5 (*a*). Because of the non-symmetric molecular structure the two nitrogen nuclei appear to be non-equivalent. At liquid nitrogen temperatures the solution in a glassy state shows distinctly separated signals related to the *z*-direction, which is perpendicular to the coordination plane, figure 5 (*b*). Due to the super hyperfine structure, the other signals are barely discernible. For the concentrated compound one broad signal is detected.

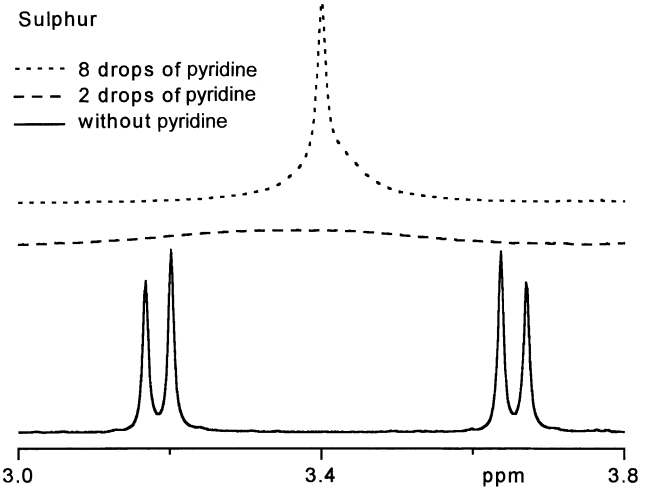

Figure 4. NMR spectra of the sulphur compound II-3 dissolved in deuterated chloroform with a small amount of deuterated pyridine.

4. Conclusions

We have synthesized nickel(II) and copper(II) complexes whose chelating centres are of very low symmetry (C_1). This chiral structure results from the chirality of the coordinating donor atoms. The chirality of the centre was detected by NMR studies for sulphur and selenium donor atoms. However, this is not

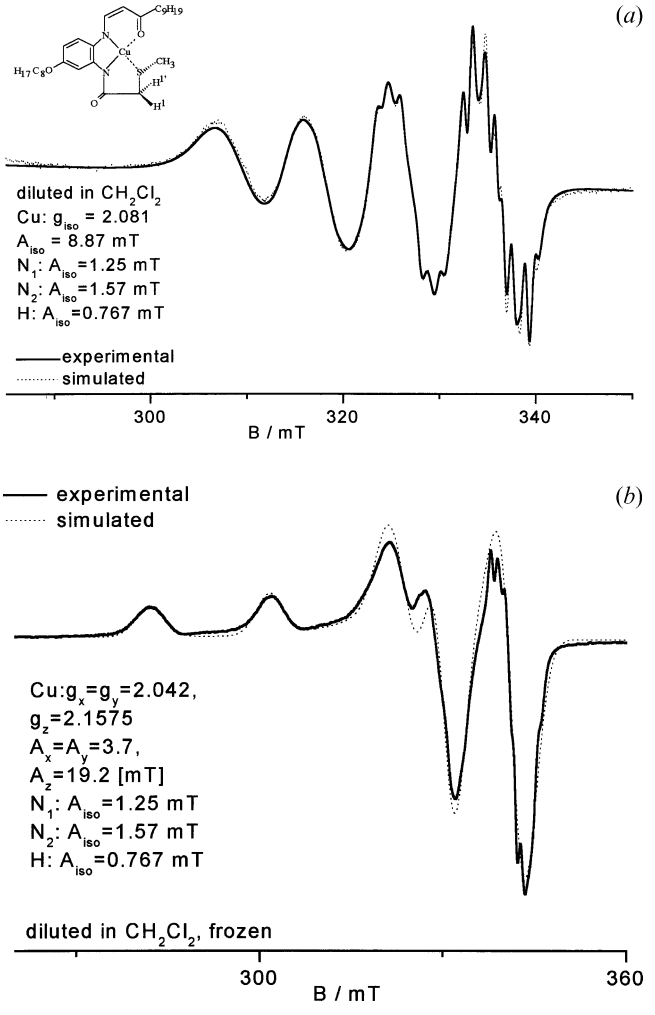

Figure 5. ESR spectra of coper complex II-1 dissolved in methylene chloride, at (*a*) room temperature, and (*b*) in liquid nitrogen.

detected for the oxygen atoms because of the too rapid inversion of the orbital configuration. It is worth noting that for the metallomesogens presented, the parent ligands are of higher C_s symmetry than the complexes obtained. The coordination bond between the donor atom and the chelated metallic ion establishes the chiral centre. However, this centre is not very stable and the enantiomeric compounds cannot be separated.

Among the compounds presented, the best calamitic phase stability was found for the mesogens with the *oxa*-butyric ring. However, a dramatic increase in the clearing temperature was observed for compounds with the *sulphur*-butyric group and with the core broadened by the phenyl ring.

Comparing the compounds presented here with those enaminoketone complexes having tetradentate ligands and forming calamitic phases synthesised previously, higher clearing temperatures are observed for the compounds with five-membered rings than for those with six-membered rings [2, 3]. This is probably due to the smaller size of the protruding core fragment — the five-membered ring gives the weaker steric hindrances from rotation around the long molecular axis than the hexagonal enaminoketone ring. An analogous promotion of rod-like phases has been found in azomethine palladium complexes containing the pentagonal L-alanine chelating ring [8] in comparison with the hexagonal acetyloacetonate ring [9–12].

References

[1] SERRANO, J. L., 1996, *Metallomesogens – Synthesis, Properties and Applications* (Weinheim: VCH).

[2] SZYDŁOWSKA, J., KRÓWCZYŃSKI, A., POCIECHA, D., PRZEDMOJSKI, J., and GÓRECKA, E., 1998, *Liq. Cryst.*, **25,** 117.

[3] SZYDŁOWSKA, J., KRÓWCZYŃSKI, A., and GÓRECKA, E., 1999, *Liq. Cryst.*, **26,** 685.

[4] BENNOUZZANE, M., COCO, S., ESPINET, P., MARTIN-ALVAREZ, J. M., and BARBERA, J., 2002, *J. mater. Chem.*, **12,** 691.

[5] GHEDINI, M., PUCCI, D., and BARBERIO, G., 2000, *Liq. Cryst.*, **27,** 1277.

[6] ROLL, C. P., DONNIO, B., WEIGAND, W., and BRUCE, D. W., 2000, *Chem. Commun.*, 709.

[7] SAMOCHOCKA, K., and GROCHOWSKI, T., 1992, *J. chem. Soc. Dalton Trans.*, 1145.

[8] HUANG, D. J., XIONG, N. Y., YANG, J., WANG, S. M., LI, G., and ZHANG, L. F., 1993, *Mol. Cryst. liq. Cryst.*, **231,** 191.

[9] GHEDINI, M., PUCCI, D., CRISPINI, A., and BARBERIO, G., 1998, *Organometallics*, **18,** 2116.

[10] GHEDINI, M., and PUCCI, D., 1990, *J. organomet. Chem*, **395,** 105.

[11] BAENA, M. J., ESPINET, P., ROS, M. B., and SERRANO, J. L., 1991, *Angew. Chem. int. Ed. Engl.*, **30,** 711.

[12] BAENA, M. J., ESPINET, P., ROS, M. B., SERRANO, J. L., and EZCURRA, A., 1993, *Angew. Chem. int. Ed. Engl.*, **32,** 1203.